Unbinding Pathway of 5-HT and Granisetron from the 5-HT_3 Receptor

A. J. Thompson[1], S. C. R. Lummis[1], P.-L. Chau[2]

[1]Department of Biochemistry
University of Cambridge
Cambridge CB2 1QW
United Kingdom
Email: pc104@pasteur.fr

[2]Author for correspondence at
Bioinformatique Structurale
Institut Pasteur
75724 Paris
France

Key words: molecular recognition, ligand-receptor interactions, 5-HT, granisetron, 5-HT_{3A} receptor, molecular dynamics simulations, site-directed mutagenesis, ligand unbinding, serotonin receptor, ligand-gated ion channel, Cys-loop receptor, neurotransmitter binding site; ligand docking, homology modelling, extracellular domain, binding loops

Abstract

We have utilised molecular modelling, molecular dynamics and mutagenesis of the 5-HT_3 receptor to predict the pathway for agonst and antagonist movement into and out of the ligand binding site. Static models of bound antagonist initially revealed interactions outside of the presumed ligand binding pocket and suggested the presence of an energy minimised state that existed between the ligand binding site and the external face of the 5-HT_3 receptor. Molecular dynamic simulations of antagonist unbinding revealed that this location existed within an unbinding pathway. Simulations of agonist unbinding highlighted the same route. Experimental evidence from mutagenesis of the 5-HT_3 receptor is consistent with the proposed entry/exit route. We conclude that agonist and antagonist access the ligand binding site in the same manner, along a pathway that is roughly 8 Å in length. The entrance to the pathway is via an opening that is located on the outside of the extracellular domain, allowing ligands to gain direct access from the extracellular environment. Similar to the binding site, the pathway lies between adjacent subunits.

Introduction

The 5-HT_3 receptor is a member of the Cys-loop ligand-gated ion channel family that also includes the nicotinic acetylcholine (nACh), glycine, $GABA_A$ and $GABA_C$ receptors. These receptors are responsible for fast synaptic transmission and are the targets of many neuro-active drugs. Each of these receptors is formed by the assembly of five subunits that surround a central ion-conducting pore. Experiments on chimaeric forms of these receptors has encouraged the view of the subunits as modular proteins that can be broken into two distinct domains (Bouzat et al., 2004; Eiselé et al., 1993; Kriegler et al., 1999; Verbitsky et al., 2003). The transmembrane domain of each subunit contains four α-helical segments (M1-M4) that cross the lipid membrane with predominantly non-polar residues of M2 lining the central ion-conducting pore. A large intracellular loop between M3 and M4 influences single channel conductance (Kelley et al., 2003). The extracellular N-terminal region is responsible for ligand-binding and contains the disulphide bond that gives the Cys-loop family its name.

To date five 5-HT_3 genes (A-E) (Niesler et al., 2003) have been reported, but only functional homomeric 5-HT_{3A} (Maricq et al., 1991) and heteromeric $5HT_{3A}/5HT_{3B}$ (Davies et al., 1999; Dubin et al., 1999) receptors have been described. The 5-HT_3 receptors are considered the oldest members of the Cys-loop family of proteins, so they provide a useful model for understanding features of the whole Cys-loop family (Reeves and Lummis, 2002).

Currently there is no crystal structure of the 5-HT_3 receptor, but the molecular structure of the closely related AChBp (Brejc et al., 2001; Celie et al., 2004) and results from cryo-electron microscopy on the nACh receptor (Miyazawa et al., 2003; Unwin et al., 2002)(New JMB unwin ref) have provided useful homologues from which to draw comparisons. In previous studies we presented a homology model of the extracellular domain of the 5-HT_{3A} homo-pentamer and generated a number of energetically favourable models of 5-HT docked into the ligand binding site (Reeves et al., 2003). In a

later study we performed similar homology based studies using the 5-HT_3 antagonist granisetron (Granisetron new paper) and used mutagenesis coupled with radio-ligand binding to either support or exclude the models we had generated. Comparison of the different models alluded to a pathway for ligand movement into and out of the ligand binding site (REF: new granisetron paper). However, the models we created were static and did not fully reflect the interaction of the ligand with its receptor.

Molecular dynamics simulations have been used to investigate the mechanism of ligand-receptor interaction (Kern et al., 1994; Rognan et al., 1994). The development of steered molecular dynamics allowed the ligand to unbind from the receptor (Leech et al., 1996) and this method has been applied to various ligand-receptor systems successfully (Grubmuller et al., 1996). However, this method requires the pre-determination of the unbinding trajectory. Previous work used molecular complexes where the unbinding trajectory was determined from experiments or where various putative unbinding trajectories are used for the simulation. To overcome this problem, the mutual repulsion method was developed to allow the ligand to explore its own unbinding trajectory (Chau, 2001). Using this method it was shown that the free energy change of unbinding could be estimated and demonstrtaed the effect of hydrophobic interactions

In the present study we extend the analysis of our previous homology models and provide both molecular dynamic and experimental evidence for the passage of agonist and antagonist from the binding site and into the extracellular surroundings.

Materials and Methods

Molecular Graphics: Ligand binding and snap-shots of molecular dynamics simulations were viewed in SwissPDBViwer () and ViewerLite ()..

Mutual repulsion simulation method: In the mutual repulsion method, the centres of mass of the ligand and the receptor are assigned "pseudo-charges". The potential (r) is difined in the form:

(ri) =

g2

|R1 − R2|

(1)

where ri is the position vector of the atom i, g is the magnitude of the pseudo-charge, R1 is the position vector of the centre of mass of the receptor, and R2 is that of the centre of mass of the ligand. The centres of mass of the ligand and the receptor are assigned "pseudo-charges" that increased linearly with time. The pseudo-charges interact with each other, but do not affect the normal electronic partial charges assigned to each atom. They repel or attract each other under rules similar to those for normal electronic partial charges, without disrupting the structure of the protein receptor. Further details of the method are described in a previous publication8. In this implementation, the method was altered slightly. The centre of mass of the receptor was no longer used, but a point directly "above" the ligand in the z-direction. The force on the protein was artificially reduced to zero to prevent the receptor from spinning.

Simulation details : Two series of simulations were carried out, one with 5-HT placed inside the binding site (homology model of the receptor and structure 4 from our previous work (Reeves, 2003 #383)) and the other with granisetron docked into the same site (structure 2 from our previous work (New gran ref). In the case of the simulation of ligands docked inside the 5-HT_3, the structure of the protein-ligand complex was minimised for 20000 steps using the zero-K minimisation method. Heavy atoms of the ligand and the protein C_α atoms were tethered and the structure heated up to 310K over

250 ps, followed by an equilibration period of 100 ps. During the unbinding process, the tethering was reduced to the C_α atoms of every five amino acids. In half the simulations, the tethering remained like this during the whole unbinding. In the other half, the tethering was lifted from the C_α atoms of the binding-site amino acids. Unbinding forces were increased from zero in a linear manner at a rate of 0.05 units per fs. The aim was to achieve an unbinding speed of about 20m/s.

Ligand docking: Granisetron was docked using AutoDock 3.05 (Goodsell and Olson, 1990; Morris et al., 1998). The binding pocket is geometrically well-defined. A 60X60X60 grid with spacing 0.375 Å was used to cover the binding pocket exclusively. 10 genetic algorithm runs were carried out to dock each of the four stereo-isomers of granisetron. For the genetic algorithm, a population size of 50 was used, and the maximum number of generations was set to 27,000. A total of 13 unique docked poses were generated. These structures were used as input for software created by one of us (PLC, see ref (Reeves et al., 2003)) that identified all amino acids that had at least one atom within 5 Å of the ligand. Potential hydrogen bonding interactions were identified using SwissPDBViewer (Guex and Peitsch, 1997).

Materials: All cell culture reagents were obtained from Gibco BRL (Paisley, U.K.), except foetal calf serum which was from Labtech International (Ringmer, U.K.). [^{3}H]granisetron (81 Ci/mmol) was from PerkinElmer (Boston, MA). All other reagents were of the highest obtainable grade.

Cell culture: Human embryonic kidney (HEK) 293 cells were maintained on 90mm tissue culture plates at 37°C and 7% CO_2 in a humidified atmosphere. They were cultured in DMEM:F12 (Dulbecco's Modified Eagle Medium / Nutrient Mix F12 (1:1)) with GLUTAMAX I™ containing 10% foetal calf serum and passaged when confluent. Cells were grown in 90-mm-diameter dishes and transfected using calcium phosphate precipitation (Chen and Okayama, 1988; Jordan et al., 1996) at 80-90% confluency. Following transfection cells were incubated for 3-4 days before assay.

Site-directed mutagenesis: Mutagenesis reactions were performed using the method described by Kunkel (Kunkel, 1985). The 5-$HT_{3A(b)}$ subunit DNA (Accession: AY605711) has been described previously (Hargreaves et al., 1994). Oligonucleotide primers were designed according to the recommendations of Sambrook *et al* (Sambrook et al., 1989) and some suggestions of the Primer Generator (ref (Turchin and Lawler, 1999); http://www.med.jhu.edu/medcenter/primer/primer.cgi). A silent restriction site was incorporated into each primer to assist rapid identification.

Radioligand Binding: This was undertaken as previously described (Lummis et al., 1993) with minor modifications. Briefly, HEK293 cells that had been transfected with wild-type or mutant DNA were washed twice with phosphate buffered saline (PBS) at room temperature. They were then scraped into 1 ml of ice-cold HEPES buffer (10 mM, pH 7.4) containing the following proteinase inhibitors (PI): 1 mM EDTA, 50 μg/ml soybean trypsin inhibitor, 50 μg/ml bacitracin and 0.1 mM phenylmethylsulphonyl fluoride. Harvested cells were washed in HEPES/PI and frozen at -20°C. After thawing, they were washed twice with HEPES buffer, resuspended and 50 μg of cell membranes were incubated in 0.5ml HEPES buffer containing [^{3}H]granisetron (81 Ci/mmol, PerkinElmer). Initially, single-point radioligand binding assays were performed using 1nM and sometimes 20nM [^{3}H]granisetron to test for specific binding. If specific binding was present, saturation binding (8 point) assays were performed on at least three separate plates of transfected cells for each mutant. Non-specific binding was typically determined by the addition of 1 μM d-tubocurarine (dTC) or 1μM quipazine (both potent 5-HT_3 receptor antagonists) which gave equivalent results (Gill et al., 1995; Lummis et al., 1993). Reactions were incubated for 1 h at 4°C and were terminated by rapid vacuum filtration using a Brandel cell harvester onto GF/B filters pre-soaked for 3 h in 0.3 % polyethyleneimine (Huang et al.) followed by two rapid washes with 4 ml ice cold HEPES buffer. Radioactivity was determined by scintillation counting (Beckman LS6000sc). Specific binding was as high as 70,000 DPM with fmol/mg protein in the range 100-2000. A typical binding curve is shown in figure 1. Protein concentration was estimated using the Bio-Rad Protein Assay with BSA standards. Data were analyzed by iterative curve fitting (GraphPad, PRISM, San Diego, CA) according to the equation:

$B=(B_{max} \cdot [L])/(K + [L])$, where B is bound radioligand, B_{max} is maximum binding at equilibrium, K is the equilibrium dissociation constant, [L] is the free concentration of radioligand.

Results

Homology Models

Docking of the 5-HT_3 antagonist, granisetron, to a homology model of the 5-HT_3 receptor previously revealed 26 energetically favourable models that could be split into three distinct groups (Granisetron REF). An example of the amino acid residues located within 5 Å of the bound antagonist for each of these groups is shown in figure 1 and reveals that groups A and B are broadly similar with the orientation of granisetron being the main distinguishing feature (see also figure 1 from GRANISETRON PAPER REF). In contrast, residues in group C occupy a different location within the 5-HT_3 homology model and the position of granisetron is unique. A comparison of the residues from groups A and B (which are essentially identical) with the residues of group C (figure 1d) show that group C amino acids lie closer the external surface of the extracellular domain than those of group A/B. Consistent with these residues representing a pathway rather than a true binding site, fewer of the residues in group C are associated with amino acids that were found to have significant effects on radioligand binding in our previous study (Granisetron binding REF). Furthermore, fewer of the group C residues have been identified as key binding residues in other members of the LGIC family (ref?? Sine review?? + others??).

Unbinding Simulations

Table 1 shows a comparison of symetric and asymetic tethered residues that lie within 5 Å of the ligand pathway during unbinding. Comparison of symetric and asymetric tethered residues shows that both methods identified similar amino acids….***ANYTHING ELSE CHAU…***

To dock 5-HT and granisetron into the 5-HT_3 receptor, ligands were allowed to equilibrate for.. and …etc… Unbinding of these ligands was performed over ?? ns and snap shots of the events taken at ??ns intervals. Figure 2 shows the location of residues within 5 Å of the ligands at varying time frames during the simulation. It can be seen that both 5-HT and granisetron are located at similar sites at the beginning of each simulation

and the orientations of the molecules are consistent with previously published observations (refs Granisetron paper, davids paper, Macksay??) – ***THIS STATEMENT NEEDS CHECKING***. As the simulation progresses both 5-HT and granisetron move along a similar vector which can be described as both down and outwards from the center of the receptor. 5-HT exits the pathway more quickly than granisetron - ***IS THIS SIGNIFICANT CHAU??***. The proposed entrance to the binding route for the two ligands is located ?? Å above the level of the membrane and allows access to a ?? Å long pathway that terminates at the ligand binding site. No other pathways were identified during our simulations. In particular, even when repulsion between the ligand and receptor was reversed and strongly directed towards the center of the extracellular domain, the ligand was unable to exit the binding site through the inner vestibule wall as has previously been hypothesised (Unwin et al REF).

Discussion

High resolution images of the ACh receptor at 9 Å initially revealed electron densities at the level of the ACh binding sites (Unwin, 1993). These were later clarified by images at 4.6 Å (Miyazawa et al., 1999) and by the presence of a ligands in the crystal structures of the AChBp (Brejc et al., 2001; Celie et al., 2004).

Earlier studies have suggested that agonist entry into the binding site would be from the outer vestibule of the receptor (Miyazawa et al., 1999) in a similar fashion to the binding route for acetylcholinesterase (Sussman et al., 1991). However, with the advent of higher resolution images it now thought that this is unlikely. In our models the binding site is accessed through a narrow pore that faces the extracellular environment and whose entrance is located roughly ?? Å above the surface of the membrane. Initially this pathway was alluded to by ligand binding simulations that were based upon 5-HT_3 homology models of AChBp. Molecular dynamic simulations have revealed that repulsion of the ligand away from the center (***or somwehere else???***) of the receptor leads to a gradual movement of the ligand from the binding site and into the extracellular space. These simulations have provided further evidence for the proposed ligand pathway. In favour of this hypothesis, the effects of mutagenesis on radioligand binding in this region are consistent with location of the pathway. Amino acid residues that are close to the binding site have been shown to have a more significant effect on radioligand binding than those that are more distant (granisetron REF). Importantly, amino acids identified within the binding pathway are different to conserved residues known to be directly involved with ligand binding in other LGIC members (Brejc et al., 2001)(Gran REF), making it unlikely that they represent residues within a ligand binding site.

Comparison of closed state and open state structures of the nACh receptor reveals that the C-loop moves upon ligand binding (Unwin, 2005). In the unbound or closed state the position of the C-loop is less obstructive to the proposed binding pathway and would allow better accessibility to the binding site. Upon binding, the C-loop moves down and partially obstructs the binding pathway. Structural details of the F-loops region are poorly

resolved in the crystal structures of the AChBp (Brejc et al., 2001; Celie et al., 2004) and in cryo-electron microscopy images of the nACh receptor (UNWIN REF), but it is possible that this region also undergoes structural changes upon ligand binding. Evidence from the 5-HT_3 receptor (Granisetron Ref and others??) and other members of the LGIC family (REFS??) have implicated the F-loop in binding, but it is possible that the effects observed in these studies were not always a direct consequence of interactions within the binding site, but may have reflected steric hindrance or disruption of transitory interactions within the ligand pathway. Although there is no direct evidence of such movement, it is possible that the F-loop reflects the action of the C-loop and partially occludes the entrance to the binding site from the opposite side. Occlusion of the binding pathway would momentarily lock the ligand in place (ANY IMPLICATIONS FOR ANTAGONIST EFFECTS???)

Acknowledgements

SCRL is a Wellcome Trust Senior Research Fellow in Basic Biomedical Sciences. PLC and SCRL thanks the Royal Society for a European Scientific Exchange Programme travel grant.

Figure Legends

Table 1 . A comparison of the effects of symmetric tethering and asymmetric tethering on the residues that lie within 5 Å of the 5-HT and granisetron unbinding pathway.

Figure 1. A comparison of residues within 5Å of the ligand binding site from groups A, B and C respectively. Granisetron is shown in blue. **1D.** A comparison of residues that are in groups A/B (Yellow) and group C (Red). Residues that are common to both groups are highlighted in orange.

Figure 2. Movements of 5-HT and granisetron during a ??ns unbinding simulation. For ease of viewing only two subunits from the pentamer are shown. **2A.** 5-HT has been equilibrated within the binding site and is then allowed to exit the 5-HT_3 receptor by ***mutual repulsion?? Utilising Aymmetric tethering??***. The location of 5-HT at ??ns (white), ??ns (grey) and ??ns (Galzi et al.) time intervals (CHAU – what are the time intervals between frames ??) is shown and reveals that the ligand moves both down and out during the unbinding process. **2B.** Granisetron has been docked and unbound using the same methods as those in 2A and exits the binding site along the same pathway as 5-HT. ***Add the directions of mutual repulsion onto a small cartoon insert???. I have made one of the models black and whote and the other colour – do you have a preference?***

Figure 3. Location of amino acid residues within the ligand binding site and proposed ligand pathway superimposed onto a 5-HT_3 homology model that includes the extracellular and transmembrane domains. **3A.** A view looking towards the receptor. **3B.** A wire view of the pentameric protein, showing the pathway from the side. The position of the membrane is shown as a light grey box in both figures.

Figure 1

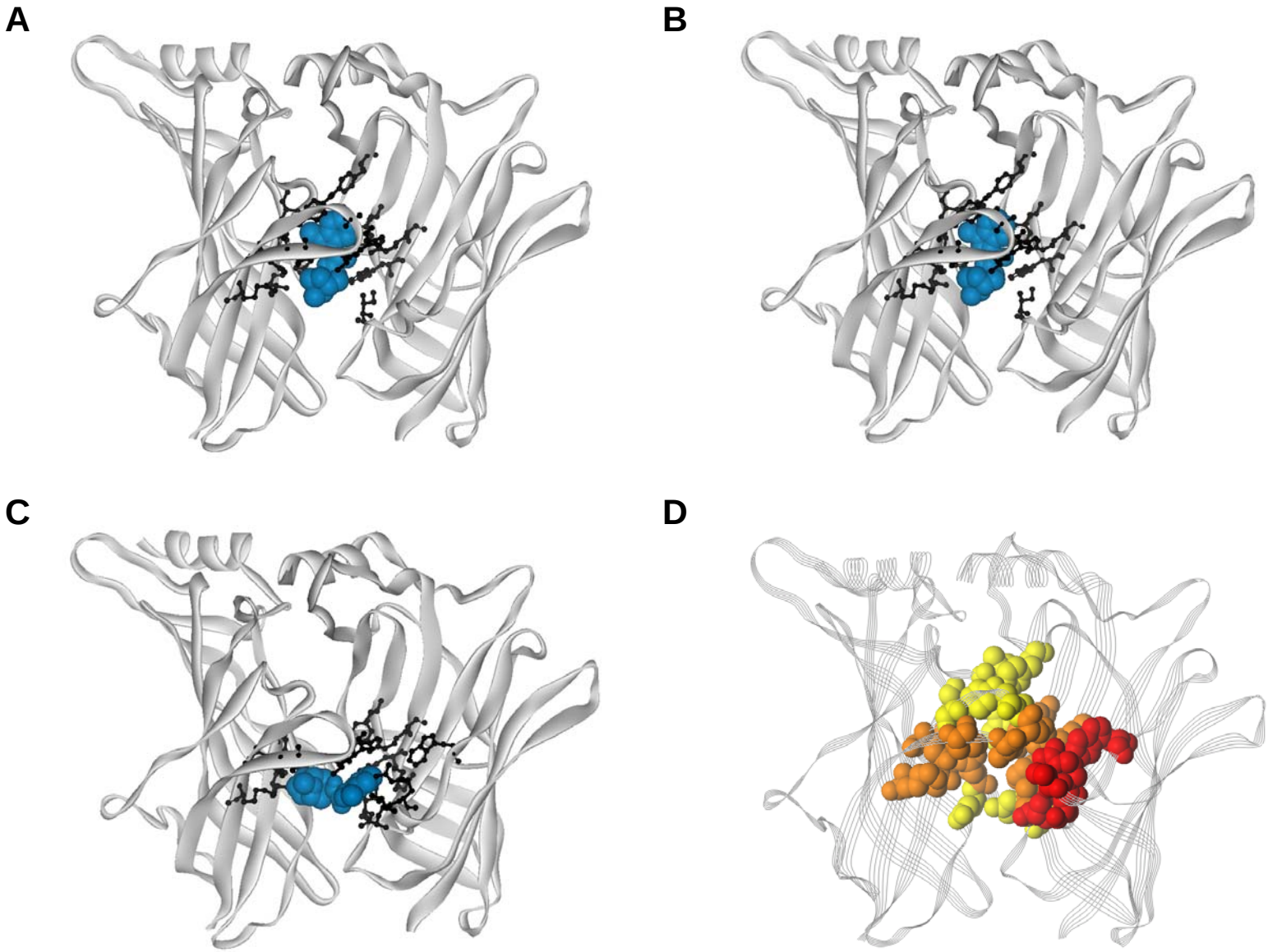

Figure 2

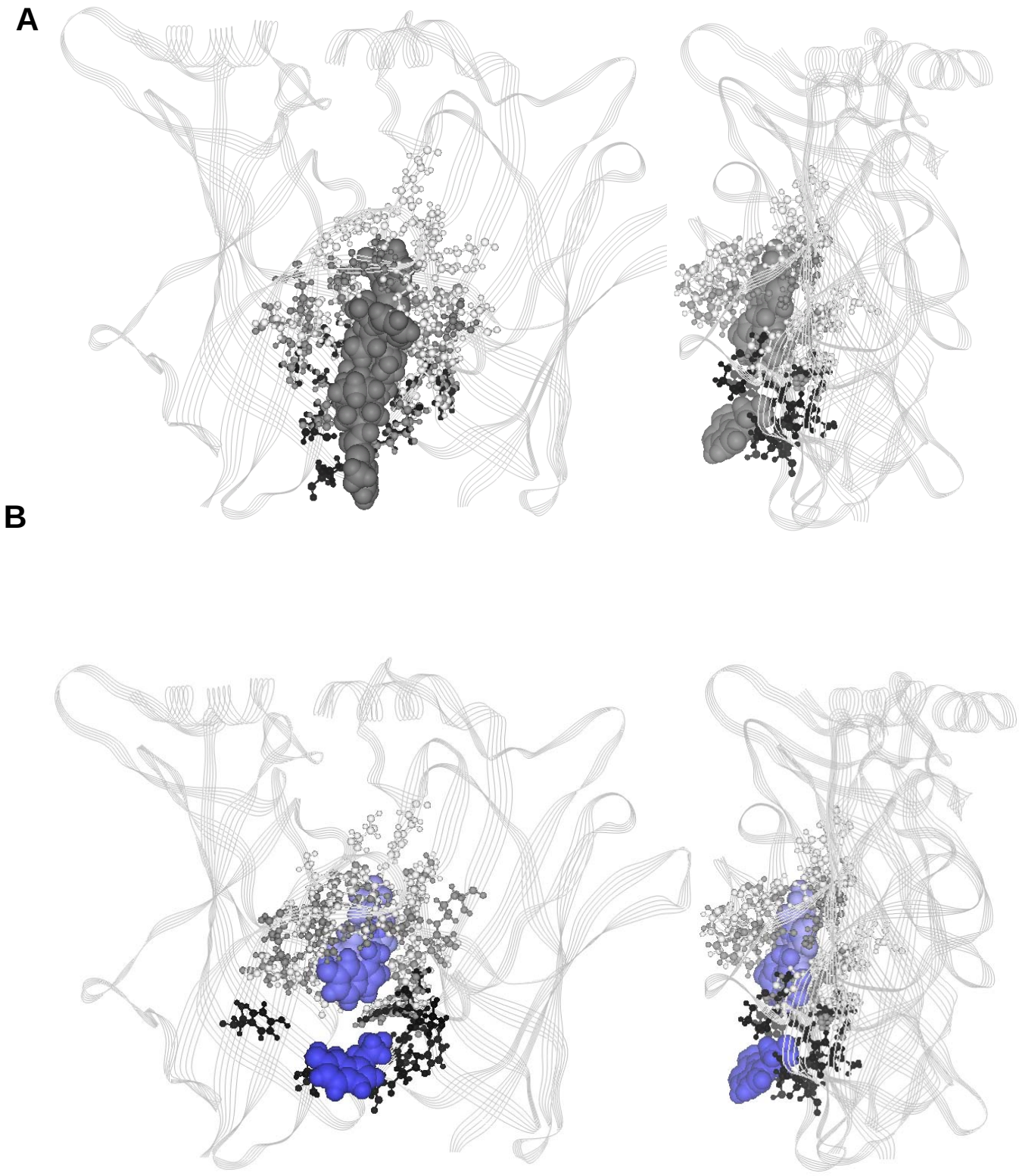

Figure 3

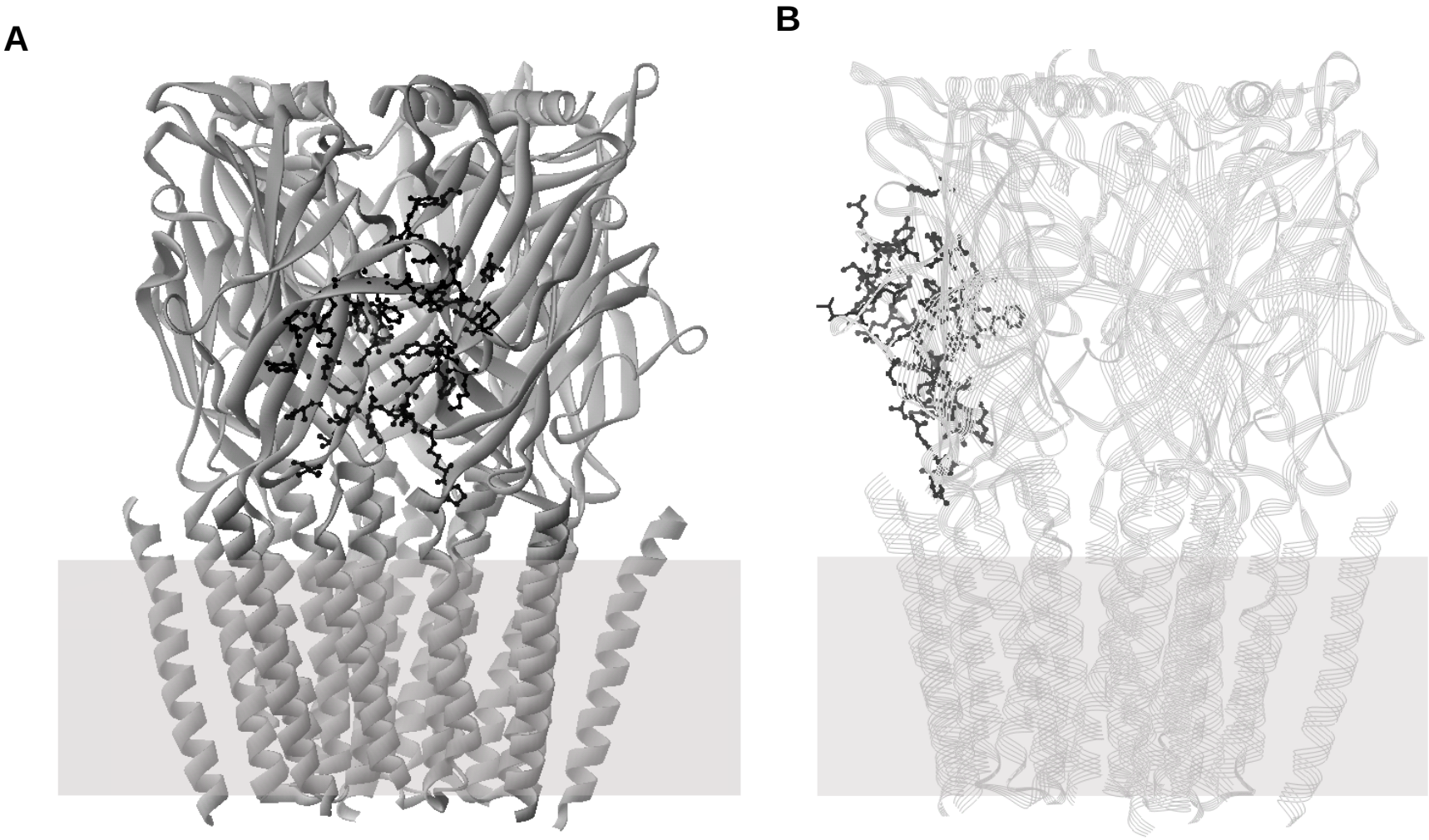

Bouzat, C., F. Gumilar, G. Spitzmaul, H.L. Wang, D. Rayes, S.B. Hansen, P. Taylor, and S.M. Sine. 2004. Coupling of agonist binding to channel gating in an ACh-binding protein linked to an ion channel. *Nature*. 430:896-900.

Brejc, K., W.J. van Dijk, R.V. Klaassen, M. Schuurmans, J. van Der Oost, A.B. Smit, and T.K. Sixma. 2001. Crystal structure of an ACh-binding protein reveals the ligand-binding domain of nicotinic receptors. *Nature*. 411:269-76.

Celie, P.H., S.E. van Rossum-Fikkert, W.J. van Dijk, K. Brejc, A.B. Smit, and T.K. Sixma. 2004. Nicotine and carbamylcholine binding to nicotinic acetylcholine receptors as studied in AChBP crystal structures. *Neuron*. 41:907-14.

Chau, P.-L. 2001. Process and thermodynamics of ligand-receptor interaction studied using

a novel simulation method. *Chemical Physics Letters*. 334:343-351.

Chen, C.A., and H. Okayama. 1988. Calcium phosphate-mediated gene transfer: a highly efficient transfection system for stably transforming cells with plasmid DNA. *Biotechniques*. 6:632-8.

Davies, P.A., M. Pistis, M.C. Hanna, J.A. Peters, J.J. Lambert, T.G. Hales, and E.F. Kirkness. 1999. The 5-HT3B subunit is a major determinant of serotonin-receptor function. *Nature*. 397:359-63.

Dubin, A.E., R.D. Huvar, M.R. Andrea, J. Pyati, J.Y. Zhu, K.C. Joy, S.J. Wilson, J.E. Galindo, C.A. Glass, L. Luo, M.R. Jackson, T.W. Lovenberg, and M.G. Erlander. 1999. The pharmacological and functional characteristics of the serotonin 5-HT3A receptor are specifically modified by a 5-HT3B receptor subunit. *Journal of Biological Chemistry*. 274:30799.

Eiselé, J.-L., S. Bertrand, J.-L. Galzi, A. Devillers-Thiéry, J.-P. Changeux, and D. Bertrand. 1993. Chimaeric nicotinic-serotonergic receptor combines distinct ligand binding and channel specificities. *Nature*. 366:479-83.

Galzi, J.L., F. Revah, D. Black, M. Goeldner, C. Hirth, and J.P. Changeux. 1990. Identification of a novel amino acid alpha-tyrosine 93 within the cholinergic ligands-binding sites of the acetylcholine receptor by photoaffinity labeling. Additional evidence for a three-loop model of the cholinergic ligands-binding sites. *J Biol Chem*. 265:10430-7.

Gill, C.H., J.A. Peters, and J.J. Lambert. 1995. An electrophysiological investigation of the properties of a murine recombinant 5-HT3 receptor stably expressed in HEK 293 cells. *Br J Pharmacol*. 114:1211-21.

Goodsell, D.S., and A.J. Olson. 1990. Automated docking of substrates to proteins by simulated annealing. *Proteins*. 8:195-202.

Grubmuller, H., B. Heymann, and P. Tavan. 1996. Ligand binding: molecular mechanics calculation of the streptavidin-biotin rupture force. *Science*. 271:997-9.

Guex, N., and M.C. Peitsch. 1997. SWISS-MODEL and the Swiss-PdbViewer: an environment for comparative protein modeling. *Electrophoresis*. 18:2714-23.

Hargreaves, A.C., S.C. Lummis, and C.W. Taylor. 1994. Ca2+ permeability of cloned and native 5-hydroxytryptamine type 3 receptors. *Mol Pharmacol*. 46:1120-8.

Huang, X., T. Liu, J. Gu, X. Luo, R. Ji, Y. Cao, H. Xue, J.T. Wong, B.L. Wong, G. Pei, H. Jiang, and K. Chen. 2001. 3D-QSAR model of flavonoids binding at benzodiazepine site in GABAA receptors. *J Med Chem*. 44:1883-91.

Jordan, M., A. Schallhorn, and F.M. Wurm. 1996. Transfecting mammalian cells: optimization of critical parameters affecting calcium-phosphate precipitate formation. *Nucleic Acids Res*. 24:596-601.

Kelley, S.P., J.I. Dunlop, E.F. Kirkness, J.J. Lambert, and J.A. Peters. 2003. A cytoplasmic region determines single-channel conductance in 5-HT3 receptors. *Nature*. 424:321-4.

Kern, P., R.M. Brunne, and G. Folkers. 1994. Nucleotide-binding properties of adenylate kinase from Escherichia coli – a molecular-dynamics study in aqueous and vacuum environments. *Journal of Computer-Aided Molecular Design*. 8:367-388.

Kriegler, S., S. Sudweeks, and J.L. Yakel. 1999. The nicotinic alpha4 receptor subunit contributes to the lining of the ion channel pore when expressed with the 5-HT3 receptor subunit. *J Biol Chem*. 274:3934-6.

Kunkel, T.A. 1985. Rapid and efficient site-specific mutagenesis without phenotypic selection. *Proc Natl Acad Sci U S A*. 82:488-92.

Leech, J., J. Prins, and J. Hermans. 1996. SMD: visual steering of molecular dynamics for protein design. *IEEE Computational Science and Engineering*. 3:38-45.

Lummis, S.C., M.I. Sepulveda, G.J. Kilpatrick, and J. Baker. 1993. Characterization of [3H]meta-chlorophenylbiguanide binding to 5-HT3 receptors in N1E-115 neuroblastoma cells. *Eur J Pharmacol*. 243:7-11.

Maricq, A.V., A.S. Peterson, A.J. Brake, R.M. Myers, and D. Julius. 1991. Primary structure and functional expression of the 5HT3 receptor, a serotonin-gated ion channel. *Science*. 254:432-7.

Miyazawa, A., Y. Fujiyoshi, M. Stowell, and N. Unwin. 1999. Nicotinic acetylcholine receptor at 4.6 A resolution: transverse tunnels in the channel wall. *J Mol Biol*. 288:765-86.

Miyazawa, A., Y. Fujiyoshi, and N. Unwin. 2003. Structure and gating mechanism of the acetylcholine receptor pore. *Nature*. 424:949-55.

Morris, G.M., D.S. Goodsell, R.S. Halliday, R. Huey, W.E. Hart, R.K. Belew, and A.J. Olson. 1998. Automated docking using a Lamarckian genetic algorithm and an empirical binding free energy function. *Journal of Computational Chemistry*. 19:1639-1662.

Niesler, B., B. Frank, J. Kapeller, and G.A. Rappold. 2003. Cloning, physical mapping and expression analysis of the human 5-HT3 serotonin receptor-like genes HTR3C, HTR3D and HTR3E. *Gene*. 310:101-11.

Reeves, D.C., and S.C. Lummis. 2002. The molecular basis of the structure and function of the 5-HT3 receptor: a model ligand-gated ion channel (review). *Mol Membr Biol*. 19:11-26.

Reeves, D.C., M.F. Sayed, P.L. Chau, K.L. Price, and S.C. Lummis. 2003. Prediction of 5-HT(3) Receptor Agonist-Binding Residues Using Homology Modeling. *Biophys J*. 84:2338-44.

Rognan, D., L. Scapozza, G. Folkers, and A. Daser. 1994. Molecular dynamics simulation of MHC-peptide complexes as a tool for predicting potential T cell epitopes. *Biochemistry*. 33:11476-85.

Sambrook, J., E.F. Fritsch, and T. Maniatis. 1989. Molecular Cloning. A Laboratory Manual. Cold Spring Harbor Laboratory Press.

Sussman, J.L., M. Harel, F. Frolow, C. Oefner, A. Goldman, L. Toker, and I. Silman. 1991. Atomic structure of acetylcholinesterase from Torpedo californica: a prototypic acetylcholine-binding protein. *Science*. 253:872-9.

Turchin, A., and J.F. Lawler, Jr. 1999. The primer generator: a program that facilitates the selection of oligonucleotides for site-directed mutagenesis. *Biotechniques*. 26:672-6.

Unwin, N. 1993. Nicotinic acetylcholine receptor at 9 A resolution. *J Mol Biol*. 229:1101-24.

Unwin, N. 2005. Refined structure of the nicotinic acetylcholine receptor at 4A resolution. *J Mol Biol*. 346:967-89.

Unwin, N., A. Miyazawa, J. Li, and Y. Fujiyoshi. 2002. Activation of the Nicotinic Acetylcholine Receptor Involves a Switch in Conformation of the alpha Subunits. *J Mol Biol*. 319:1165-76.

Verbitsky, M., P.V. Plazas, and A.B. Elgoyhen. 2003. Functional expression and properties of a nicotinic alpha9/5-HT3A chimeric receptor. *Neuroreport*. 14:1931-4.